SHORT COMMUNICATIONS

"Natural" Hydrogen and Acoustic Emission in Kh18N10T Steel after Barocryodeformation

E. V. Chernyaeva[a], A. M. Polyanskii[b], V. A. Polyanskii[b]*, P. A. Khaimovich[c],
Yu. A. Yakovlev[b], and D. L. Merson[d]

[a] St. Petersburg State University (Staryi Petergof branch), Universitetskii pr. 28, Staryi Petergof, St. Petersburg, 198504 Russia
[b] R & D Corporation Electronic and Beam Technologies, Bronevaya ul. 6, St. Petersburg, 198188 Russia
*e-mail: vapol@electronbeamtech.com
[c] Kharkov Institute of Physics and Technology, National Scientific Center, Akademicheskaya ul. 1, Kharkov, 61108 Ukraine
[d] Tol'yatti State University, Belorusskaya ul. 14, Tol'yatti, 445667 Russia
Received October 5, 2009; in final form, December 3, 2009

Abstract—Hydrogen with different bond energies and indentation-induced acoustic emission in the initial (homogenized) state of Kh18N10T stainless steel and after barocryodeformation by 18 and 31% are studied. A correlation between the acoustic parameters and the hydrogen content in the material is found.

DOI: 10.1134/S1063784210070236

The hydrogen accumulated in a metal in the course of production, working, and use of steel products considerably influences the mechanical properties of the metal. Concentrating inside the metal in traps with different hydrogen bond energies in them, the hydrogen, having a different diffusibility, may influence the strength and plasticity of the material [1]. Therefore, when designing metallic constructions, one should take into account the variation of the hydrogen concentration along with the hydrogen bond energy distribution.

It is known that a hydrogen-induced change in the mechanical state of a metal has an influence on acoustic emission (AE) [2, 3]. This effect is extremely sensitive: a change even in the "natural" concentration of hydrogen, which is usually as low as several hydrogen atoms per several hundreds of thousands of host metal (matrix) atoms, may alter its parameters [4, 5].

To improve the physicomechanical properties of metals and alloys is a challenging problem of materials science. A promising approach in this respect seems to be barocryodeformation (BCD): plastic deformation of a material under high hydrostatic compression at cryotemperatures [6]. BCD makes it possible to produce a highly dispersed structure and thereby improve the strength of the metal [7, 8].

In this work, we study the effect of BCD on the content of dissolved hydrogen and on the AE parameters in Kh18N10T stainless steel in the initial state (after homogenizing annealing at 1050°C followed by water quenching) and after BCD by 18 and 31% at 77 K.

Measurements of the hydrogen content and the distribution of hydrogen over bond energies were made by high-temperature vacuum extraction using an AV-1 hydrogen analyzer [9]. A sample was heated in the vacuum chamber of the analyzer to desired temperatures (see table) and then the hydrogen content was analyzed using a mass-spectrometric technique combined with recording of an extraction curve (the time dependence of the amount of extracted hydrogen). After each measurement, the extraction system without the sample was heated to the next temperature point and the sample was simultaneously cooled inside the instrument in the absence of air. Then, the procedure was repeated. Such an approach makes it possible to eliminate background hydrogen flows from the extraction chamber walls, which arise when the temperature of the chamber varies.

The discrete thermodiffusion spectrum thus obtained shows how the amount of released hydrogen depends on the extraction temperature. The sum of discrete values equals the total content of hydrogen in the sample. From this spectrum, one can estimate the hydrogen content distribution over bond energies, find the temperature at which the sample becomes fully outgassed, determine the degree of outgassing in a technological process, etc. Since hydrogen evolves from steels in the molecular form, the bonding energy is defined as the activation energy of diffusion per hydrogen molecule.

When the sample is heated to 250°C, the hydrogen adsorbed on its surface liberates first. At temperatures in the range 350–550°C, diffusible hydrogen (with a bond energy below 0.8 eV) is released, and strongly bonded hydrogen (with a bond energy above 1 eV) evolves at temperatures above 550°C. It follows from the table that the amount of the hydrogen adsorbed on the surface increases and the amount of the diffusible hydrogen decreases with increasing the BCD level. In

Amount Q of extracted hydrogen in the initial state and after BCD

Extraction temperature, °C	Initial state	BCD 18%	BCD 31%
	Q, ppm	Q, ppm	Q, ppm
250	0.151	0.369	0.599
350	0.381	0.143	0.151
450	0.399	0.298	0.282
500	0.329	0.116	0.166
550	0.284	0.423	0.185
700	0.365	0.203	0.451
850	0.061	0.135	0.867
Amount of hydrogen adsorbed on surface	0.151	0.369	0.599
Amount of diffusible hydrogen (bond energy below 0.8 eV)	1.393	0.980	0.785
Amount of strongly bonded hydrogen (bond energy above 1 eV)	0.426	0.338	1.317
Total amount of hydrogen in sample	1.970	1.687	2.701

addition, the thermodiffusion spectrum of hydrogen evolution changes upon BCD.

While the hydrogen evolution curve taken of the sample in the initial state is more or less smooth (Fig. 1, curve *1*), the curve taken upon 18% BCD (Fig. 1, curve *2*) exhibits distinct maxima at 450 and 550°C and that taken after 31% BCD (Fig. 1, curve *3*) peaks at 450 and 850°C. Upon heating to 900°C or higher, the heavily deformed sample becomes completely outgassed at a higher temperature than the undeformed and weakly deformed samples. This means that strong deformation increases the amount of hydrogen captured by traps with a high binding energy.

The structure examination and magnetometric studies showed that the samples after homogenizing annealing have a homogeneous austenite structure with grains ≈50 μm across. Dislocations in the samples are distributed randomly with a mean surface density of ~10^9 cm^{-2}. Homogenized Kh18N10T steel shows the tendency for the transformation of initial γ-austenite (fcc lattice) into α-martensite (bcc lattice). The magnetometry data and the results of X-ray investigation of the phase composition indicate that the martensite content reaches 90% or more when the BCD varies from 25% to 45%.

During deformation, phase transformations proceed in the sequence γ ⟶ ε ⟶ α, where ε-martensite is an intermediate phase with an hcp lattice. The steel deformed by 16% contains ε-martensite lamellas alternating with α-martensite grains and some amount of residual austenite. The microdiffraction data suggest that the ε-martensite lamellas contain a large number of thin deformation stacking faults and the α-martensite has a subgranular structure with subgrains often having an elongated shape and varying in size from 0.01 to 0.25 μm. The misorientation of subgrains

inside a grain is considerable and achieves 7°. Dislocations inside subgrains are distributed nonuniformly, and their mean density falls into the range 5×10^9–8×10^{10} cm^{-2}. At a degree of reduction of 33%, the ε-phase almost completely transforms into α-martensite. As a whole, the microstructure of the sample becomes finely dispersed and equiaxial. The mean dislocation density reaches ~10^{11} cm^{-2}.

The martensite thus obtained ages at 300−500°C: intermetallides precipitate at the boundaries of martensite cells, considerably pinning the boundaries. As a result, the yield stress and tensile strength grow. As the temperature rises above 600°C, the martensite obtained by deformation transforms into austenite.
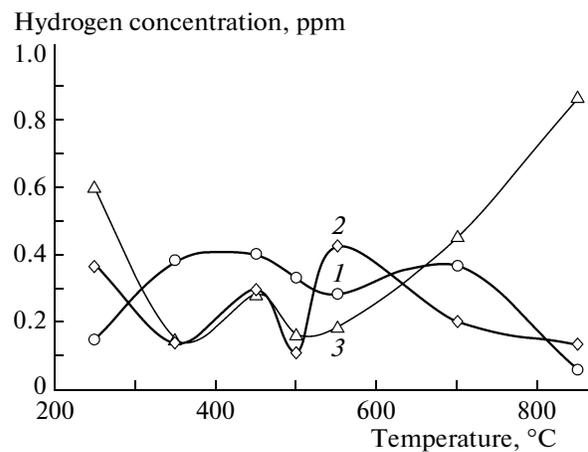

Fig. 1. Extraction temperature dependence of the amount of hydrogen evolved from Kh18N10T steel (*1*) in the initial state and after BCD by (*2*) 18% and (*3*) 31% (discrete TDS).
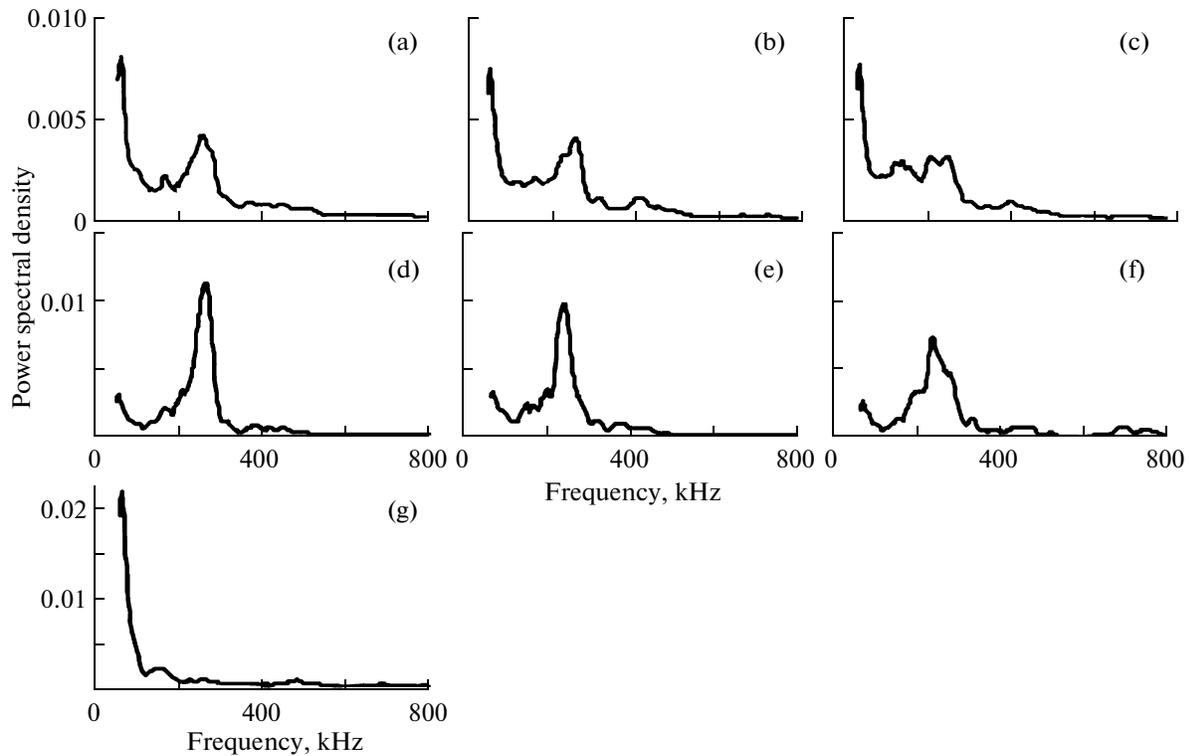
Fig. 2. Main types of signals from the samples of Kh18N10T steel (a, d, g) in the initial state and deformed by (b, f, g) 18% and (c, f, g) 31%: (a–c) type I, (d–f) type III, and (g) type II. Barocryodeformation resulted in the widening and lowering of signals I and III, 31% deformation often causing bifurcation of signals I (see (c)). In addition, signals III in the deformed samples are slightly shifted toward lower frequencies. Signals II remained unchanged for all the samples. Finally, as the deformation grows, AE signals become more uniform; that is, the percentage of signals I increases reaching 85%.

Based on the aforesaid, one can suppose that the narrow hydrogen evolution peak (at 450°C) observed in the sample subjected to BCD (Fig. 1) is related to martensite aging and the $\alpha \longrightarrow \gamma$ transition liberates strongly bonded hydrogen.

These structural evolutions and their related hydrogen redistributions change the acoustic properties of the samples.

Acoustic emission was initiated by indenting a hard-alloy conic indenter on an IM-4A mechanical test machine. The maximal indentation load was 1000 N.[1] AE signals were detected with an MSAE-L2 sensor and converted to electrical signals with an MSAE-FA010 amplifier with a total gain of 87 dB. All recorded AE signals were divided into groups according to the shape of the power spectral density curve by the technique described in [10], and spectral portraits (the averaged shape of the power spectral density curve) were analyzed.

Three basic groups of signals were distinguished. The first group was the largest (65–85% of all records). It included low-energy signals with three peaks in the curve (Figs. 2a–2c). They will be referred to as type-I signals. High-energy low-frequency signals (Fig. 2g) and signals with one distinct peak (Figs. 2d–2f) will be referred to as type-II and type-III signals (in order of decreasing percentage; type-III signals accounted for 5–10%).

Let us compare "smooth" and acoustic results (Fig. 3). It is seen that the behavior of hydrogen with different bond energies distinctly correlate with quantitative AE data.

(i) As the degree of BCD increases, the content of diffusible hydrogen with a bond energy of less than 0.8 eV (Fig. 3, curve *3*) drops and the amount of hydrogen adsorbed on the surface (curve *4*) rises. The total number of signals (curve *5*) decreases.

(ii) In the sample deformed by 31%, the total amount of released hydrogen (curve *1*) increases drastically because of the evolution of strongly bonded hydrogen with a bond energy of higher than 1 eV (curve *2*). Simultaneously, the AE uniformity, i.e., the percentage of main (type-I) signals, rises (curve *7*). The small increase in the uniformity is explained by a low hydrogen content (below 3 ppm).
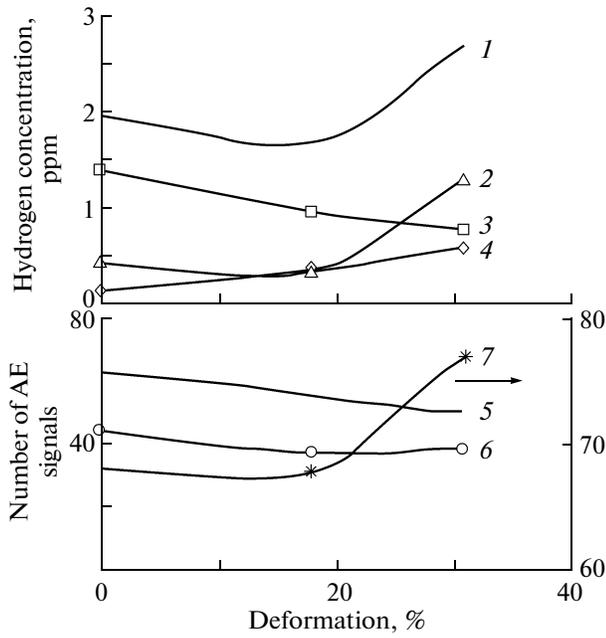
---

[1] Usually, the ductility of metals is studied with loads varying between 1 and 10 N. However, in the case at hand, a dislocation density necessary for AE detection is not reached at such loads. Therefore, we conduct analysis in terms of macrohardness and consider a correlation between AE and the influence of hydrogen concentration on deformation processes in a macrovolume.

Fig. 3. Hydrogen content and parameters of AE emission vs. the degree of BCD for the samples of Kh18N10T steel. (*1*) Total content of hydrogen, (*2*) content of strongly bonded hydrogen, (*3*) content of diffusible hydrogen, (*4*) content of hydrogen adsorbed on the surface, (*5*) total number of AE signals, (*6*) number of type-I signals, and (*7*) percentage of type-I signals.

(iii) Aging and decomposition of nanostructured elements upon heating are accompanied by hydrogen evolution into the environment.

Thus, the amount of hydrogen in terms both of concentration and of bond energy depends on the structure of Kh18N10T steel after BCD, which may have a considerable effect on the final mechanical properties of a metal. The samples under study were not saturated by hydrogen. All the effects described here were observed at low (natural) concentrations. It is found (as in [4, 5] for 35G2 and 20 steels) that the AE parameters correlate with the content of hydrogen with different bond energies; that is, they can serve as a metal state indicator.

REFERENCES

1. B. A. Kolachev, *Hydrogen Fragility of Metals* (Metallurgiya, Moscow, 1985) [in Russian].

2. V. V. Zabil'skii and S. G. Il'ina, Fiz. Met. Metalloved. **90** (6), 105 (2000).

3. H. Hagi and Y. Hayashi, J. Soc. Mater. Sci. Jpn. **37**, 1442 (1988).

4. D. L. Merson, et al., Zavod. Lab., No. 2, 57 (2008).

5. E. V. Chernyaeva, et al., in *Proceedings of the 5th International Scientific Conference "Strength and Destruction of Materials and Designes," Orenburg, 2008,* Vol. 1, pp. 292–298.

6. P. A. Khaimovich, in *Proceedings of the 5th International Scientific Conference "Strength and Destruction of Materials and Constructions," Orenburg, 2008*, Vol. 1, pp. 33–39.

7. P. A. Khaimovich, Russ. Phys. J. **50**, 1079 (2007).

8. A. V. Mats and P. A. Khaimovich, Fiz. Tekh. Vys. Davlenii **19**, 69 (2009).

9. *Hydrogen Analyzer AV-1*, TU-14321–001–27480175–02, NPK EPT Certificate No. 23477–02.

10. D. L. Merson, A. A. Razuvaev, and A. Yu. Vinogradov, Defektoskopiya, No. 7, 37 (2002).